Supporting Information for "Precise, self-limited epitaxy of ultrathin organic semiconductors and heterojunctions tailored by van der Waals interactions"

Bing Wu,[1,†] Yinghe Zhao,[2,†] Haiyan Nan,[2,†] Ziyi Yang,[1] Yuhan Zhang,[1] Huijuan Zhao,[1] Daowei He,[1] Zonglin Jiang,[1] Xiaolong Liu,[1] Yun Li,[1] Yi Shi,[1,*] Zhenhua Ni,[2] Jinlan Wang,[2,3]* Jian-Bin Xu,[4] & Xinran Wang[1,*]

[1]*National Laboratory of Solid State Microstructures, School of Electronic Science and Engineering, and Collaborative Innovation Center of Advanced Microstructures, Nanjing University, Nanjing 210093, China*

[2]*Department of Physics, Southeast University, Nanjing 211189, P. R. China*

3Synergetic Innovation Center for Quantum Effects and Applications (SICQEA), Hunan Normal University, Changsha 410081, China

[4]*Department of Electronic Engineering and Materials Science and Technology Research Center, The Chinese University of Hong Kong, Hong Kong SAR, P. R. China*

* Correspondence should be addressed to X. W. (xrwang@nju.edu.cn), Y. S. (yshi@nju.edu.cn) or J. W. (jlwang@seu.edu.cn)

† These authors contribute equally to this work.

1. SLOMBE of C_8-BTBT, PTCDA and heterojunctions

We used mechanically exfoliated graphene and BN on 300nm SiO_2/Si as the epitaxy substrate. Before growth, the graphene and BN sheet was characterized by optical microscope and AFM to obtain the thickness and topological information. The growth of C_8-BTBT and PTCDA was carried out in a home-built single-zone vacuum tube furnace. We placed the C_8-BTBT source powder in the centre of the heating zone and the graphene and BN downstream. We used a turbo molecular pump to evacuate the quartz tube to ~4×10^{-6} Torr. We then heated up the source powders to a target temperature (110~120°C for C_8-BTBT, 270~280°C for PTCDA) to start the growth. To achieve SL epitaxy of monolayer PTCDA as shown in Fig. 4, the graphene substrate was placed 2~4 cm away from the centre.

2. AFM, KPFM, Raman spectroscopy, polarization-dependent absorption and PL measurements

AFM (both regular and high-resolution) and KPFM were performed on an Asylum Cypher under ambient conditions. We used Asylum ARROW UHF tips for high-resolution AFM.

Raman spectroscopy was performed on a LabRAM HR800 Raman system with 514nm laser excitation. The Raman mapping in Fig. 2 was performed on a WITec Alpha 300R confocal Raman system with a 532nm laser excitation (spot size ~300nm, laser power 1mW).

PL measurement was performed on a LabRAM HR800 Raman system with 514nm laser excitation (the laser power at sample is kept below 10μW).

Polarization-dependent absorption measurement was performed on a WITec Alpha 300R system with two linear polarizers (one between illumination source and sample, and the other between sample and detector), and without the notch filter. The two polarizers were

approximately cross-polarized to minimize the background signal of SiO_2. White light was illuminated on the sample through a 50× objective lens, and the reflected light was collected by a CCD camera through a spectrometer. The images were obtained by scanning the sample with step size of 500nm. We plotted the images by integrating the spectrum from 520 to 550nm.

3. Details of MD calculations

The MD simulations are performed in GROMACS-5.0.1 package[1] under the ensemble of constant particle number, volume, and temperature. The time step of 1 fs and cut-off distance of 1.5 nm are used. Outside the range, the smoothed particle mesh Ewald sum is applied to deal with the long-range coulomb interaction[2]. The temperature is controlled by using the berendsen thermostat and periodic boundary conditions are employed to avoid the edge effects.

The force field parameters are obtained by using AnteChamber PYthon Parser interface[3] on the basis of all-atom AMBER99SB force field[4], which can be found in supporting information. The interlayer interaction is described by combining Lennard-Jones 12-6 and Coulomb potentials:

$$E = \sum_{i=1}^{M}\sum_{j=1}^{N}[\frac{(C_i^{(12)} C_j^{(12)})^{1/2}}{r_{ij}^{12}} - \frac{(C_i^{(6)} C_j^{(6)})^{1/2}}{r_{ij}^{6}}] + k_e \frac{q_i q_j}{r_{ij}} \quad (1)$$

where $C^{(12)}$, $C^{(6)}$ and q represent atomic vdW parameters and partial charge, respectively; r is the interatomic distance and k_e is the electrostatic constant.

4. Device fabrication and measurements

To fabricate the device in Fig. 5, we started by exfoliating graphene on 300nm SiO_2/Si substrate. We then transferred a 100nm thick Au electrode to cover part of the graphene as

bottom electrode. PTCDA (~6nm) and C_8-BTBT (~9nm) were grown on the graphene sequentially. Finally we transferred another Au film on C_8-BTB as the top electrode. The transfer of Au electrode was performed under an optical microscope using a tungsten probe tip attached to a micro manipulator[7].

Electrical measurements were carried out by an Agilent B1500 semiconductor parameter analyser in a probe station under ambient condition. The photoresponse characteristics were investigated under 514nm laser excitation. The laser (spot size ~1μm) was focused on the sample with a 50× objective (NA=0.5).

5. Additional data of C_8-BTBT and PTCDA

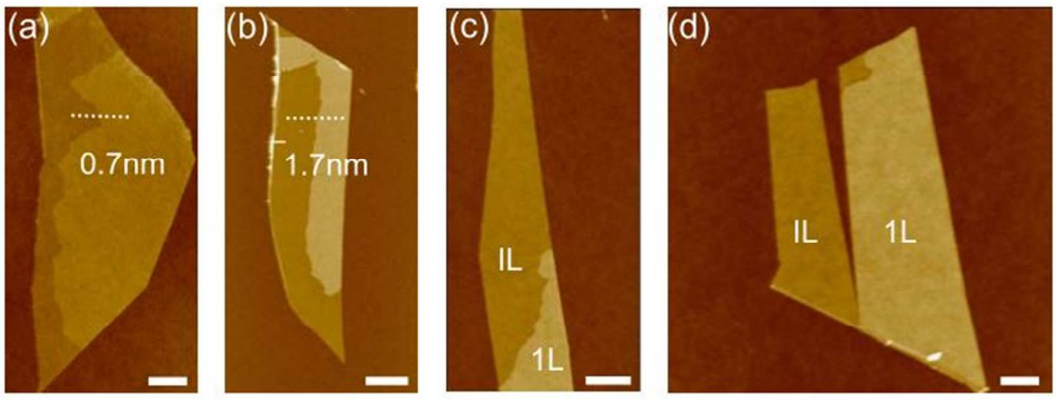

Figure S1. Layer-dependent thickness of C_8-BTBT grown on graphene. AFM images of C_8-BTBT grown on graphene, along with thickness measurement of (a)IL and (b)1L. (c)-(d) AFM images of two other incomplete 1L C_8-BTBT on IL/graphene. Scale bars: 1μm (a, d) and 2μm (b, c).

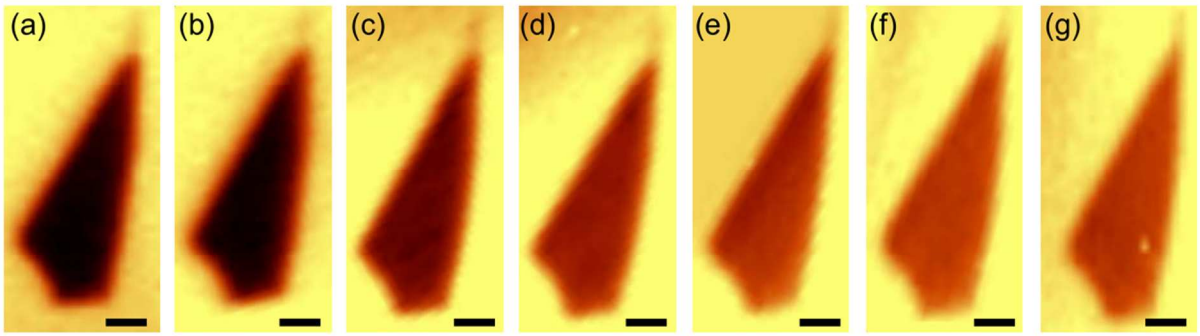

Figure S2. Polarization-dependent absorption images of the same sample in Fig. 2c. With respect to (a), the sample is rotated by (b) 15°, (c) 30°, (d) 45°, (e) 60°, (f) 75° and (g) 90°, respectively. As we rotate the sample, the absorption is uniformly modulated, confirming the single-crystalline nature of the C_8-BTBT film. All scale bars are 2μm.

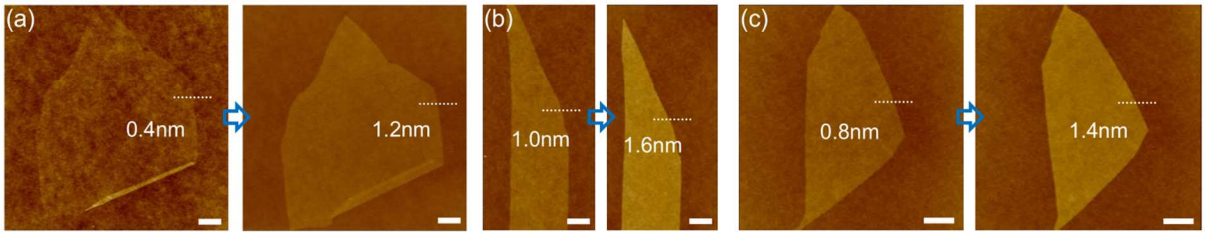

Figure S3. Three C_8-BTBT samples placed in the same position (10cm away from the center) in Zone I with different growth times. AFM images of a graphene before (left) and after (right) growth for (a) 5 minutes, (b) 10 minutes and (c) 20 minutes, respectively. The increase of thickness by 0.6~0.8nm indicates the complete coverage of monolayer C_8-BTBT on graphene in all three cases. Scale bars are 1μm for (a) and (b) and are 2μm for (c).

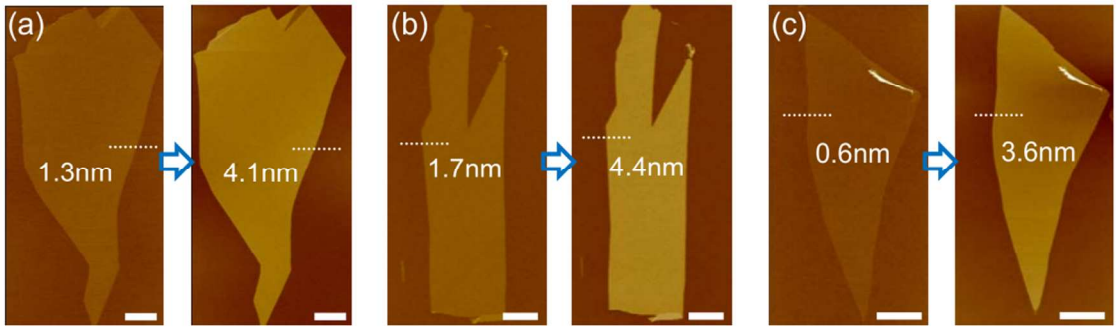

Figure S4. Three C_8-BTBT samples placed in the same position (12cm away from the center) in Zone II with different growth times. AFM images of a graphene before (left) and after (right) growth for (a) 5 minutes, (b) 10 minutes and (c) 20 minutes, respectively. The increase of thickness by 2.7~2.8nm indicates the complete coverage of bilayer C_8-BTBT on graphene in all three cases. Scale bars are 3μm for (a) and are 2μm for (b) and (c).

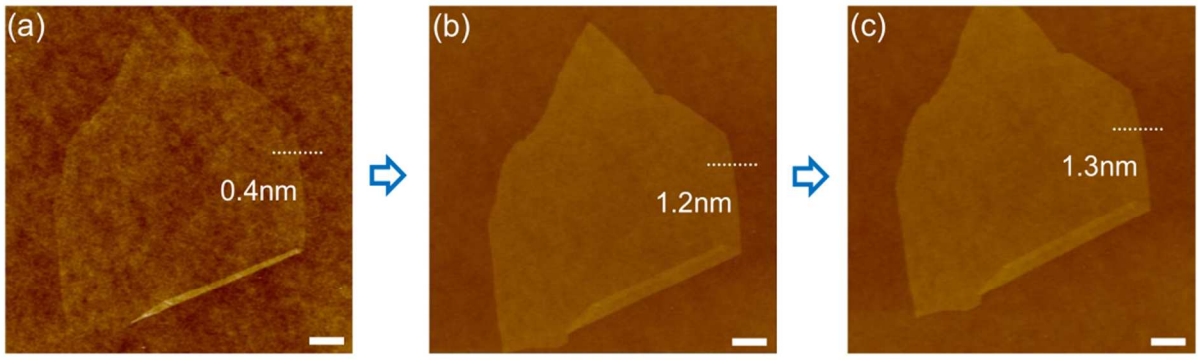

Figure S5. A monolayer C_8-BTBT sample undergone repeated growths. (a) AFM image of (a) the graphene before growth, (b) after growth in Zone I (10cm away from the center) for 5minutes and (c) after we repeat the growth for 5minutes. The repeated growth did not result in additional layers. Scale bars are 1μm.

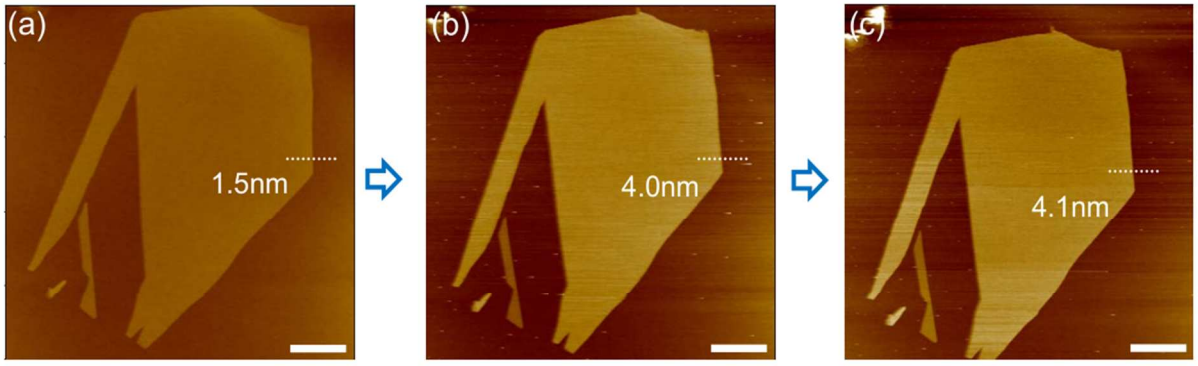

Figure S6. A bilayer C_8-BTBT sample undergone repeated growths. (a) AFM image of (a) the graphene before growth, (b) after growth in Zone II (12cm away from the center) for

5minutes and (c) after we repeat the growth for 5minutes. The repeated growth did not result in additional layers. Scale bars are 4μm.

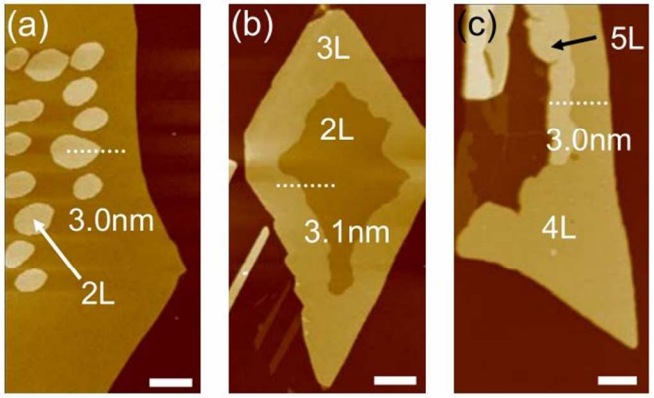

Figure S7. AFM images of three samples showing the constant height of 2L, 3L and 5L C_8-BTBT. Scale bars are (a)2μm, (b)1μm and (c)1μm.

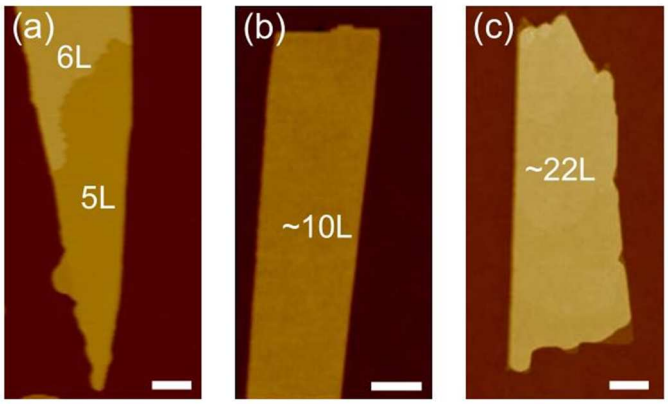

Figure S8. AFM images of uniform thicker films of C_8-BTBT and PTCDA. (a) A multi-layer C_8-BTBT grown on BN substrate. The BN was placed 13cm away from the center under 110℃ for 20 minutes. (b) A multi-layer PTCDA grown on graphene substrate. The graphene was placed 15cm away from the center under 270℃ for 15 minutes. (c) A multi-layer PTCDA grown

on graphene substrate. During growth, the graphene was placed 14cm away from the center under 270℃ for 20 minutes. Scale bars are 1μm.

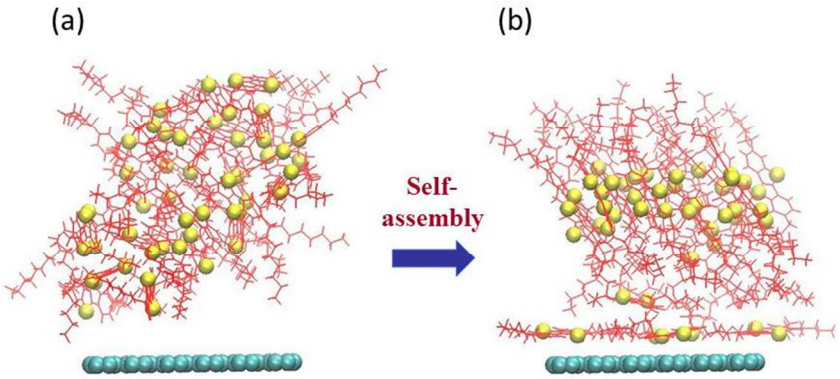

Figure S9. C_8-BTBT self-assembly on graphene at 400 K. (a) and (b) are initial and equilibrium configurations, respectively. The sulfur atoms of C_8-BTBT are highlighted for clarity.

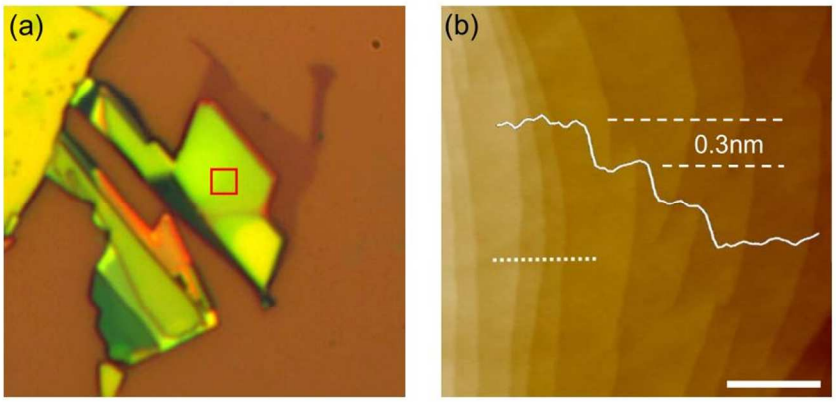

Figure S10. (a) Optical microscope images of a graphene sample after growth of bulk PTCDA (~100nm thick). (b) AFM image of the marked region in (a). PTCDA adopts layered structure with the thickness of each layer ~0.3nm, indicating face-on packing. Scale bar is 500nm.

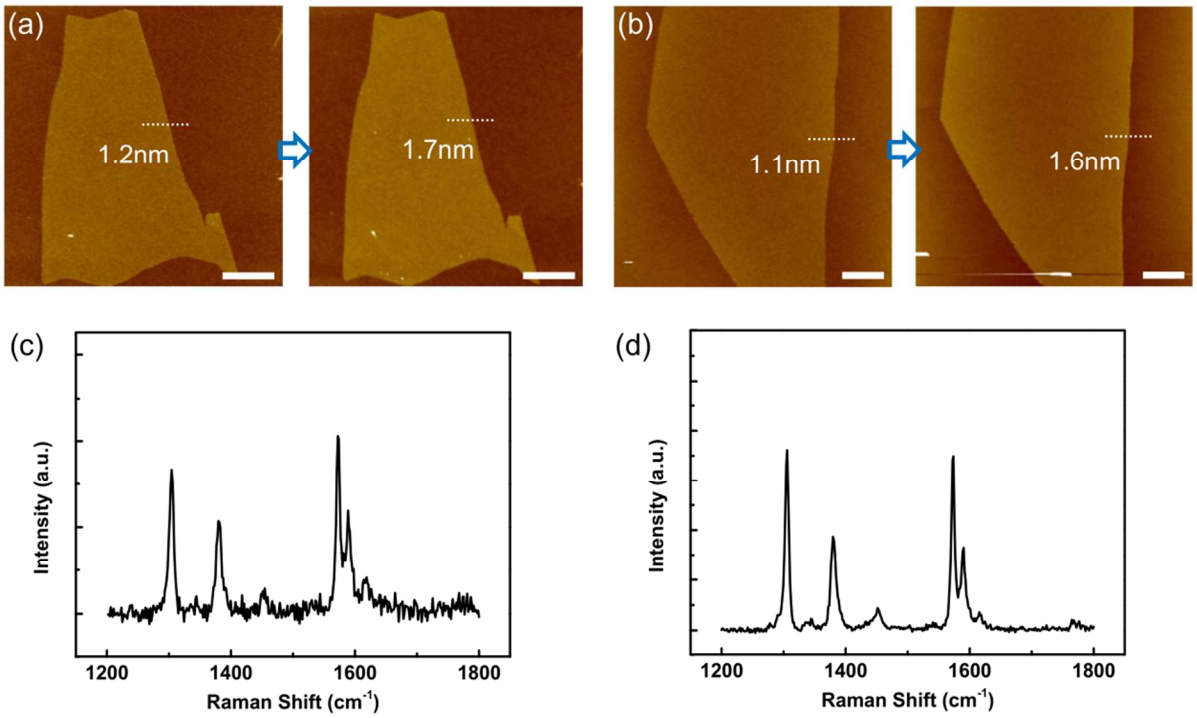

Figure S11. Two PTCDA samples placed in the same position (2cm away from the center) with different growth times. The growth temperature is 280°C for both cases. (a) AFM images of a graphene before (left) and after (right) growth for 5 minutes. After growth, the thickness of the sample was increased by ~0.5nm as expected for monolayer PTCDA. Scale bars are 1.5µm. (b) AFM images of a graphene before (left) and after (right) growth for 30 minutes. With respect to (a), longer growth time did not result in additional layers. Scale bars are 3µm. (c) Raman spectrum of the sample in (a), showing clear Raman fingerprints of PTCDA. (d) Raman spectrum of the sample in (b).

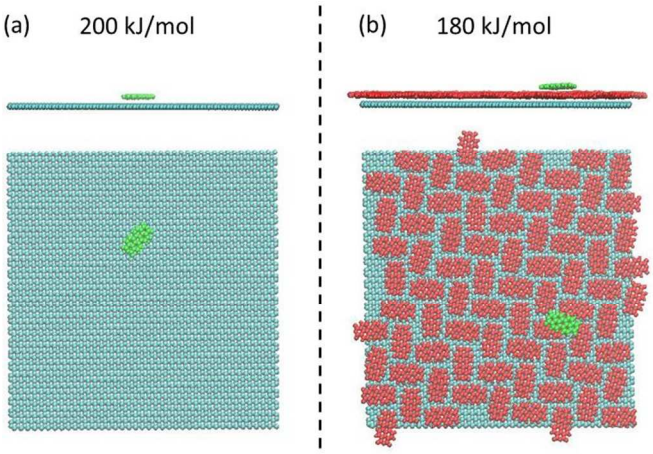

Figure S12. Binding energies and configurations of PTCDA on graphene (a) and IL/graphene (b).

REFERENCES

[1] Hess, B., Kutzner, C., van der Spoel, D., Lindahl, E. *J. Chem. Theory Comput.*, **4**, 435−447(2008).

[2] Essmann, U., Perera, L., Berkowitz, M. L., Darden, T., Lee, H., Pedersen, L. G. *J. Chem. Phys.*, **103**, 8577−8593(1995).

[3] Wang, J. M., Wang, W., Kollman, P. A., Case, D. A. *J. Mol. Graph. Model.*, **25**, 247-260(2006).

[4] Sousa da Silva, A. W., Vranken, W. F. *BMC Research Notes*, **5**, 367(2012).

[5] Sorin, E. J., Pande, V. S. *Biophys. J.*, **88**, 2472−2493(2005).

[6] Guy, A. T., Piggot, T. J., Khalid, S. *Biophys. J.*, **103**, 1028-1036(2012).

[7] Zhang, Y. H. *et al. Phys. Rev. Lett.*, **116**, 016602(2016).